crystals

MDPI

Review

Radiation Damage in Macromolecular Crystallography—An Experimentalist's View

Helena Taberman

Department of Biochemistry, University of Oxford, South Parks Road, Oxford OX1 3QU, UK; helena.taberman@bioch.ox.ac.uk

Received: 5 March 2018; Accepted: 24 March 2018; Published: 4 April 2018

Abstract: Radiation damage still remains a major limitation and challenge in macromolecular X-ray crystallography. Some of the high-intensity radiation used for diffraction data collection experiments is absorbed by the crystals, generating free radicals. These give rise to radiation damage even at cryotemperatures (~100 K), which can lead to incorrect biological conclusions being drawn from the resulting structure, or even prevent structure solution entirely. Investigation of mitigation strategies and the effects caused by radiation damage has been extensive over the past fifteen years. Here, recent understanding of the physical and chemical phenomena of radiation damage is described, along with the global effects inflicted on the collected data and the specific effects observed in the solved structure. Furthermore, this review aims to summarise the progress made in radiation damage studies in macromolecular crystallography from the experimentalist's point of view and to give an introduction to the current literature.

Keywords: X-ray radiation damage; macromolecular crystallography; dose; global damage; site specific damage; radicals

1. Introduction

Macromolecular crystallography (MX) has been the most employed technique to solve three-dimensional structures of proteins at atomic resolution to date. Since the beginning of the field, a major obstacle in MX has been the radiation damage caused by the absorption of the X-ray radiation by the crystals during the diffraction experiments. The earliest published study on MX radiation damage was in 1962 [1] and, since then, efforts have been made to understand the physical and chemical phenomena behind the observed damage and its rates, but questions still remain to be answered. These issues will be brought into even sharper focus with the current development of the more brilliant fourth generation synchrotron sources. This will necessitate structural biologists to become even more aware of the effects of radiation damage on diffraction data and on the macromolecular structures derived from them.

Free radicals are generated when X-rays are absorbed by macromolecular crystals. These radicals propagate changes that manifest in two ways: as global effects and as site specific structural changes. Global radiation damage is observed as a loss of diffraction intensity, with the weakest higher resolution reflections fading first, an increase in unit-cell volume, and higher Wilson *B*-factors, all due to the overall increase in non-isomorphism in the crystal [2–4]. These effects can preclude structure solution by, for example, causing both deterioration in the quality of the resulting electron density and incompleteness of the data. On the other hand, site specific damage, which also contributes to the global effects, is seen in the electron density maps following structure refinement. Specific damage manifests, for example, as elongation and breakage of disulphide bonds, decarboxylation of aspartic acid and glutamic acid side chains, disordering of methionine sulphurs, and photoreduction of metal centres [2,3,5–9]. Active sites and crystal contacts are particularly sensitive to specific damage [10–12],

and it can give rise to several issues: generate inaccuracies in the solved structure, disrupt experimental phasing, mislead time-resolved experiments, and even lead to incorrect biological deductions being made from the resultant structural model [13–15].

There are several stages during the crystallographic pipeline at which a structural biologist should consider how to avoid or mitigate radiation damage when planning their crystallisation and data collection steps. Furthermore, the possible effects of radiation damage should be taken into account when solving the final structure and interpreting the results. Strategies for reducing the effects of ionizing X-ray radiation have been successful, in particular, when cryocooling techniques were introduced into MX [16–19]. Holding the crystal at cryogenic temperatures (around 100 K) during X-ray data collection can reduce the rate of radiation effects by approximately 70-fold [20]. In addition, using small molecule compounds as scavengers to interact with radicals caused by the X-rays to make them less reactive has been studied, but the results have been contradictory [21]. Careful planning of the best possible data collection strategy for every case is worthwhile in order to optimize the quality and quantity of the collected data [22,23], as at cryotemperatures radiation damage increases proportionally with absorbed dose [24]. Dose is the energy per mass absorbed by the sample (J/kg = gray, Gy) and the upper experimental dose limit for a sample held at 100 K, where the total summed average diffraction intensity drops to 0.7 of the original value, was determined to be $D_{0.7} = 3.0 \times 10^7$ Gy after which the data are likely to be significantly compromised [25]. This should also be one of the factors considered when planning experimental procedures. However, it is important to realise that although it is unlikely that the crystal will give good diffraction beyond 30 MGy, data quality may well be compromised at much lower doses, since chemical factors may speed up the damage rate [11]. Dose is used as the metric against which to plot various parameters to monitor the radiation damage effects in the measured diffraction data. It is notable that when collecting data from cryocooled crystals, the global damage is proportional to dose, but not the dose rate (in units of Gy/s) [25,26]. This implies that if the same crystal is irradiated with the same X-ray beam using an oscillation angle of 1° and an exposure time of 10 s per image, then compared to using a 0.1° oscillation angle with a 1 s exposure time per image, the absorbed dose, and therefore the damage, would be the same. Specific damage has been shown to have a small measurable dose-rate effect [27].

Below is a summary of some of the ongoing efforts over the past 15 years to establish strategies for reducing the occurrence and manifestation of radiation damage from the bird's-eye view of an experimental structural biologist.

2. Crystallisation

Before there is any X-ray irradiation involved in the structure solving experiment, there are other parameters on the MX pipeline to be considered with respect to radiation damage. If the experimentalist has successfully produced a sufficient quantity of pure (preferably $\geq$ 95%) and homogeneous target macromolecule, the first step in the structure determination pipeline is to grow an ordered single crystal, and this stage can often turn out to be the bottleneck in solving the three-dimensional structure.

There are many factors that influence crystallisation, for example, pH and temperature, but the most important in terms of later radiation damage effects are the reagents used in crystallisation, either in the crystallisation solution, as small molecule additives, as detergents or in subsequent crystal soaking experiments. Inclusion of heavy metal compounds, for example, cacodylate buffer which contains arsenic, into the crystal along with the reagents will make it considerably more sensitive to radiation damage owing to the high X-ray absorption cross-section and the electron affinity of metals [28]. The atomic absorption coefficient increases approximately as the fourth power of the atomic number [29], which also means that any endogenous heavy atoms in the macromolecule will increase the amount of absorbed radiation and the macromolecule will then suffer more from radiation effects. This should also be kept in mind when choosing a purification buffer for the sample, since several contain excessive quantities of heavier elements, for example, sulphur in ammonium sulphate buffer.

Addition of small molecule compounds, scavengers, to the crystal by co-crystallisation or soaking experiments has also been studied. Scavengers intercept or interact with the radicals formed in the crystal to make them less reactive. However, the advantages of including such compounds are unclear. There are several studies which report conflicting evidence of their efficacy at mitigating radiation damage [30–33], and only one study has proved it beneficial during room-temperature data collection [34]. In the worst-case scenario, inclusion of metal containing scavengers and crystallisation reagents will merely add to the heavy atom content of the crystal and increase its X-ray absorption, making it more sensitive to radiation damage. The concentrations of several common heavy element containing reagents at which, if they were added to the crystal, the absorbed dose would double have been computed by calculating dose-doubling values using 12.7 keV incident X-rays as an example [35]. In conclusion, if avoiding elements with high absorption cross-section is not an option in purification or crystallisation of the protein, using the lowest possible concentration or replacing the reagent with a lower atomic number element containing reagent is advisable to minimize the absorbed dose.

A larger protein is likely to contain a greater number of potential sites of damage, however, other factors, such as which residues partake in crystal contacts and the presence of radiation-sensitive hotspots (e.g., active sites), appear to dictate the overall robustness of a crystal to global radiation damage. Consequently, no clear correlation between molecular weight and susceptibility to radiation damage has been established.

The minimum crystal size for MX experiments, from which it is possible to collect a complete diffraction data set prior to the onset of destructive radiation damage, has also been hypothesised theoretically as being 1.2 μm in diameter for a perfect spherical lysozyme crystal [36]. In theory, this can be reduced to 0.34 μm if photoelectron escape (defined in Section 4.1) is taken into account. This is relevant, because new serial crystallography applications are emerging and micro-sized X-ray beams are becoming common, so micro-sized crystals are usable.

3. Cryocrystallography

Once the crystallisation experiment has been successful, a decision on whether to collect diffraction data at cryogenic temperature (around 100 K) or at room temperature must be taken. Cryocrystallography combined with the data-collection method of choice, for example, multi- or single-wavelength anomalous dispersion/diffraction (MAD or SAD respectively), is still the most common practice when measuring diffraction data. In fact, 90% of the structures deposited in the Protein Data Bank (as at 25 September 2017) were determined below 160 K [37]. However, macromolecules have been shown to lose some of their conformational states and functionality with cooling, distorting results, for example, in catalysis, ligand binding, allosteric regulation and time-resolved studies [38,39]. Therefore, the rise in serial crystallographic techniques at synchrotrons and X-ray free-electron lasers (XFEL) has made room temperature measurements more popular and accessible again [40,41]. Nevertheless, cryocooling the crystal usually increases the crystal lifetime in X-ray measurements up to 100 times by reducing the mobility of most of the radicals formed during X-ray irradiation [19,42].

Prior to cooling, the crystal must be cryoprotected and, furthermore, cooled as quickly as possible to prevent the formation of ice within the sample. Protection is achieved either by replacing some of the water in the crystallisation solution by cryoagent, which can be, for example, glycerol, various different sugars, an organic solvent, a higher salt concentration or small molecular weight polyethylene glycol, or by coating the crystal with oil [18]. However, increasing the salt concentration might also potentially increase the metal concentration in the crystal and thus add to the absorbed dose and hence the damage. The cryoprotected crystal is then flash-cooled by plunging it into liquid nitrogen, or nowadays more rarely into liquid propane, or into the gaseous cold nitrogen gas stream on the X-ray apparatus [18,43] prior to data collection.

4. Diffraction Data Collection

4.1. Mechanisms of Radiation Damage

When a 100 µm thick metal free protein crystal is irradiated with an X-ray beam of 13.0 keV (wavelength of ~1 Å) in fact only approximately 3% of the radiation will interact with the crystal, which means that most of the incident beam will pass straight through it [29] as calculated by RADDOSE-3D [44,45]. This small proportion of interacting radiation can either give rise to the desired elastic and coherent Thomson (also called Rayleigh) scattering (6.5%) resulting in the diffraction pattern, or it can deposit its energy within the crystal. This occurs through Compton scattering (6.6%) or the photoelectric effect (remaining 86.9% of the interacting radiation). These different X-ray scattering processes are illustrated in Figure 1. When the incident X-ray photon interacts with an atom in the crystal, the phenomenon is called primary damage. Note that the processes by which X-rays interact with the crystal and their relative probabilities are dependent on the energy of the incident beam [28].

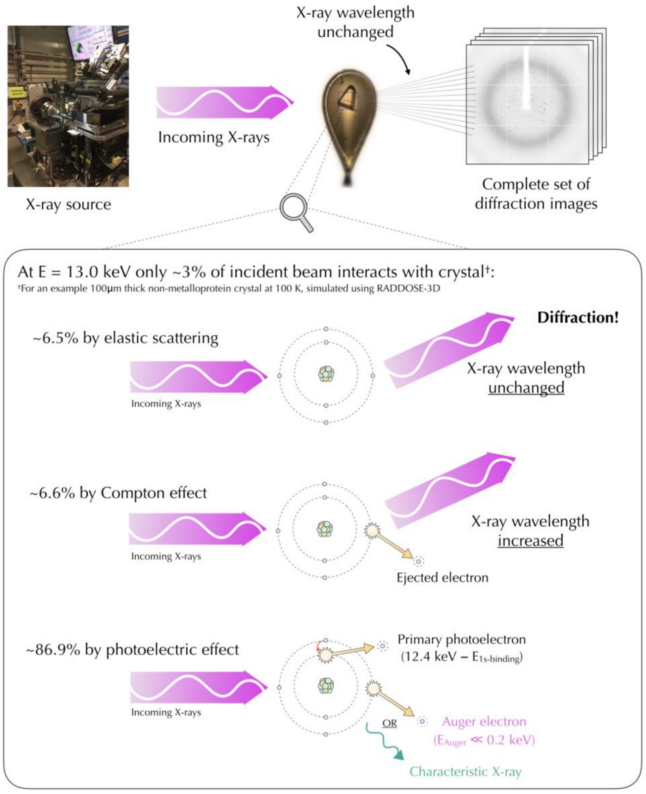

Figure 1. The different primary X-ray scattering processes of an incident 13.0 keV beam with an example lysozyme crystal simulated using RADDOSE-3D [44,45]. Elastic scattering (6.5% of the interacting beam): the X-ray photon is scattered, resulting in diffraction. Compton scattering (6.6% of the interacting beam): the photon loses part of its energy in an atomic electron, being scattered at a longer wavelength. A recoil electron may then be ejected from the atom. Photoelectric absorption (86.9% of the interacting beam): the photon transfers all its energy to an inner shell electron, which is ejected from the atom (photoelectron). The resulting orbital vacancy is filled by a higher shell electron, followed by either the fluorescence emission or ejection of a lower energy Auger electron. The X-ray source in the figure is Diamond Light Source beamline I03.

In the inelastic incoherent Compton effect, the X-ray scatters from an atomic electron in the crystal and loses part of its energy to the electron, the so-called recoil electron, which then may be ejected from the atom [46]. At higher incident X-ray energies (>20 keV) the probability of Compton scattering increases and this process can cause damage in the macromolecule. However, at lower

incident energies, the Compton effect contributes only minimally to the total damage [28], but does increase the background on diffraction images.

The major process of absorption of X-rays by macromolecular crystals is the photoelectric effect, in which the interacting photon transfers all of its energy to an atomic electron. This high-energy photoelectron is then ejected from the inner electron shell of an atom creating a vacant site, which will be filled with a higher shell electron, simultaneously releasing excess energy. When using microcrystals, the photoelectron may even escape out of the crystal [47]. The ejection of the photoelectron from the atom is followed by either emission of X-ray fluorescence or of a lower energy Auger electron, to carry away the excess energy and return the atom to its ground state. The probability of fluorescence emission increases with atomic number and becomes greater than 10% for $Z \leq 18$, being, for example, 34% for iron ^{56}Fe [48]. Every photoelectron that is produced is able to migrate for a few micrometres from its original site in the crystal, giving rise to a cascade of up to 500 more ionisation events (for 12.4 keV X-rays) including formation of hydroxyl radicals, protons, hydrogen atoms and electrons [46,47,49,50]. This phenomenon is called secondary damage. All the primary and secondary ions, radicals and electrons can either directly alter the macromolecule itself (direct damage) or the surrounding solvent (indirect damage).

At cryotemperatures the mobility of most of the radicals is significantly reduced, as discussed above, but it has been shown through electron spin resonance studies that electrons are mobile even at 77 K [51] and they are presumed to be the main cause of radiation damage in 100 K MX experiments [49]. In addition to all the electrons that are formed as a result of the interactions described above, electron loss centres, i.e., positive holes, are also generated simultaneously in the crystal. These holes are believed to be mobile at 100 K, but more easily trapped than electrons.

4.2. Data Collection Methods

Next, the data collection method which is going to be used to derive the phases from the diffraction data needs to be defined [52]. This will determine the energy of the incident X-ray beam and the quantity of data required. The initial decision depends on whether a homologous structure with a sufficient sequence identity (approximately $\geq$30%) exists, which can be used as a template for molecular replacement (MR) phasing, the most commonly used method for solving the phase problem [53]. If a previously solved suitably similar structure is available, usually only one complete data set measured with a wavelength of approximately 1 Å is adequate to solve the three-dimensional structure of the macromolecule of interest. The biggest drawback in using molecular replacement as the phasing method is model bias: i.e., the new structure will be biased in favour of the structure used as the MR model.

If MR is not an option or is unsuccessful, experimental phasing methods must be considered. Many of the remaining phasing methods in question depend on the scattering signal contributed by the electrons of either intrinsic or added heavy atoms, and finding their positions, while simultaneously preserving isomorphism between data sets. These include different isomorphous replacement and anomalous diffraction techniques and their combinations [54].

In isomorphous replacement, several data sets from multiple isomorphous crystals are collected, one from a native crystal and at least one from a heavy atom derivative. The change in intensities between the data sets (measured at a common λ of ~1 Å) is then used to deduce the positions of the heavy atoms in the macromolecule, for example, using the SHELXC and D software [55,56]. This does require co-crystallization or most often soaking of heavy metal compounds into the macromolecule crystal, which naturally means an increase in absorbed radiation when diffraction data are measured. When soaking for heavy metal derivatization is required, a very high excess of metal containing reagent is added into the crystallisation mother liquor. Afterwards, backsoaking, i.e., soaking again to a non-heavy metal containing solution, can be used to remove non-bound heavy atoms that do not contribute to the diffraction signal, but would again increase the X-ray absorption [57]. In addition to the increased X-ray absorption, the added heavy metal may also cause changes in the unit cell (non-isomorphism) or even crystal degradation. Furthermore, finding a suitable concentration and

soak time for the heavy atom reagent is an exhaustive trial and error process. Careful data collection from the heavy metal derivative crystal is needed: the absorbed dose should stay as low as possible and the multiplicity should be high for the data to be useful for isomorphous phasing. This means that particular attention should be paid to the photon flux and exposure time used during data collection.

Nowadays the most common experimental phasing methods are the anomalous dispersion techniques, in which either the natively present sulphur atoms or heavier elements and incorporated selenomethionines can be used as a source of anomalous signal to determine the phases using only one crystal. Phases are solved using the dispersive differences between at least two data sets from the same crystal measured at several different wavelengths (MAD) or between multiple measurements of the Friedel-related reflections from the same crystal at the same wavelength (SAD) [58]. These methods also set requirements for the synchrotron beamline, since it must be tuneable to enable the wavelength to be changed between datasets. The most important wavelength to use to collect a data set for MAD or SAD phasing is at (or at least very close to) the absorption peak of the particular heavy metal, where the maximum anomalous differences between Bijvoet pairs will be obtained. Unfortunately, when measuring data near or at the metal's absorption edge, the crystal will absorb even more of the incident radiation than when collecting below the edge, so the radiation damage rate will be higher than for a native crystal.

When comparing MAD and SAD methods, the quantity of data gained with MAD is much higher and it is less dependent on sample characteristics, which will usually result in more accurate overall electron density maps [59]. On the other hand, the disadvantage of MAD is that after collecting the first complete data set at least a second data set needs to be collected, which again increases exposure time and absorbed dose proportionally. Furthermore, due to the unit cell expansion and site-specific damage increase with dose, the non-isomorphism between the data sets measured at different wavelengths increases, which causes challenges later when processing the data [60]. SAD experiments have been said to be superior compared with MAD experiments. The data collection time is significantly shorter, and concentrating on collecting an accurate data set at the energy of maximum anomalous differences can make SAD more effective and radiation damage robust [61]. This can be changed by choosing the parameters of a two-wavelength MAD experiment carefully, for example, considering in what order to use the selected wavelengths [62].

Radiation damage itself can also be used as a phasing method by utilizing the specific structural changes in the macromolecule inflicted by X-rays [63]. In radiation-damage-induced phasing (RIP) several data sets are collected from a single crystal: first a complete low-dose data set is obtained, followed by a 'burn' with an unattenuated beam up to approximately 10 MGy dose, after which a second low-dose data set is collected. Phases are derived from the specific changes between the two low-dose data sets, for example, the broken disulphide bridges and the new conformations of the sulfides. RIP alone might not give enough information for obtaining accurate phases, but it is certainly powerful when combined with, for example, S-SAD [64].

4.3. Data Collection Parameters

There are several aspects to take into account in the practical implementation of the data collection. Firstly, the beam characteristics have a significant effect. When collecting diffraction data from metalloproteins the choice of beam energy is pivotal, since heavy metals absorb radiation significantly more when irradiated on and above their absorption edge [11]. When considering the effects of incident X-ray energy on a native, non-metal-containing protein, there have been several systematic studies, but no clear consensus on whether the beam energy has an effect on the rate of the radiation damage has been established [7,65–68]. The beam size used to collect the data should ideally be matched to the crystal size [69]. This decreases the interactions with the surrounding crystallisation reagents and consequently also reduces the background. If the beam size is smaller than the crystal, the resulting diffraction intensity will be lower [70,71].

The importance of the beam profile should also be recognized as having an effect on radiation damage manifestations. A top-hat profile beam is ideal in order to illuminate the crystal uniformly with the same flux across the irradiated volume and will result in a similar rate of damage throughout the crystal [37]. However, most commonly the beam shape has an approximately Gaussian profile, resulting in inhomogenous irradiation of the crystal. The more intense flux at the peak of the beam causes damage faster than the tails of the Gaussian shaped flux distribution [72]. The experimenter should aim to achieve a top-hat beam profile, for example, by defocusing the beam and using slits to reduce its size.

Knowledge of the beam (energy, flux, size, and profile) along with prior knowledge of the macromolecule crystal (size, shape, orientation relative to the incident beam, number of heavy atoms in solvent and protein, unit cell parameters and the number of residues) and data collection specifics (oscillation range and exposure time) allow the absorbed dose to be calculated with RADDOSE-3D [44,45].

Choosing the data collection protocol wisely is also worth the effort. In addition to serial crystallography, which should be used for the smallest crystals, composite data collection for multiple crystals [73] and helical scans for rod shaped crystals [74] are an option to consider. The data collection should have a clear objective and the parameters adjusted accordingly. For example, the exposure time of an image, beam transmission and the size of the data collection wedge are directly related to the resolution and completeness of the resulting data set.

5. Structure Solution and Interpretation

After the diffraction experiment, the data will have to be processed with, for example, XDS [75] or the DIALS [76] software packages. Any signs of global damage in reciprocal space will make this more difficult, decreasing the resolution limit and completeness of the data and making their scaling and merging more complicated. Therefore, the resulting electron density maps will be significantly noisier. Several global damage indicators can be plotted against absorbed dose to study radiation damage effects, for example, the decay of the average summed intensity of the data set over the initial average summed intensity (I_n/I_1), the unit cell volume, and the relative scaling *B*-factor [29,37]. The processed data are then phased using the chosen method. After a set of structure factor amplitudes and their phases have been derived, the electron density map can be calculated for each point in the asymmetric unit. The map may be degraded due to the issue mentioned above regarding the beam profile, when a Gaussian shaped beam results in non-uniform irradiation of the crystal, inducing a mixture of inhomogeneously damaged conformational states across the crystal. The map will show the average over all these states.

Next, an atomic model of the macromolecule is built into the electron density according to its sequence. Even if all the necessary radiation damage precautions have been taken before and during the data collection, it is quite possible that the crystal will nevertheless have suffered some specific radiation damage. At cryotemperatures, specific damage can occur up to 60 times faster than any signs of radiation damage can be detected from the diffraction images [35]. This can compromise the biological conclusions being drawn from the solved structure. Interestingly, specific damage to susceptible amino acid residues, which manifests as changes in the electron density maps, is not the same over the whole structure, but varies from one susceptible atom or group to another, for example, according to their local environment, indicating that it is an effect of secondary radicals [4,77]. This can be observed, for example, in the specific order that the disulphide bonds in lysozyme are cleaved. A multi-track model has been used to explain this phenomenon [78].

In addition to the site-specific effects listed above, tyrosine has been previously reported to suffer specific radiation damage by possible cleavage of the side chain carbon-oxygen bond [5], but this has recently been disproved. A cleavage event is energetically extremely improbable, and instead the tyrosine undergoes conformational change due to breakage of surrounding hydrogen bonding networks [79]. As mentioned above, active site residues appear to be particularly susceptible to specific

radiation damage [12,15,80]. This is thought to be because of the chemical and geometric strains to which these residues are subject [2,10]. As active sites are usually the most interesting part of the structure, this can make the biological information, for example, enzymatic mechanism, be compromised and care in the interpretation must be exercised. Naturally, the intrinsic metals of metalloproteins also absorb a greater number of X-rays making these proteins more sensitive to radiation damage and causing changes in the oxidation states of the metal centres [6]. This happens at doses over three orders of magnitude lower than the 30 MGy 100 K experimental dose limit [37]. Due to the radiation sensitivity of metalloproteins, combining MX studies with complementary spectroscopic methods is important when studying the structure and reaction mechanism of metalloproteins. Care must be taken to reduce the effects of radiation damage by irradiating the metalloprotein crystal at an X-ray wavelength away from (and if possible below) the absorption edges of any metals present in the sample. Choosing composite data collection or serial crystallography should be considered to minimize or even prevent radiation-induced redox modifications [81]. In addition, collecting the diffraction data of a metalloprotein at 40 K has been shown to decrease metal reduction 30-fold compared to irradiation at 110 K [8].

In contrast to the X-ray induced specific damage in proteins, less is known about the effects in crystals of nucleic acids and their protein complexes. Recently nucleic acids in DNA-protein and RNA-protein complex crystals have been shown to be significantly more durable and robust to radiation, but they do suffer from the cleavage of base sugar nitrogen-carbon and sugar-phosphate carbon-oxygen bonds [82,83].

Specific damage can be studied and visualised by calculating Fourier difference density maps between observed structure factors obtained from data sets collected from the same crystal and the same data collection wedge [84]. This results in information on electron density loss and gain sites in the macromolecule as a function of dose. Examples of difference density maps for specific damage sites are presented in Figure 2. Using the Radiation-Induced Density Loss (RIDL) script [85] to calculate per atomic metrics for the electron density change, it is also possible to track the time-dependent changes in the crystallographic data. RIDL also highlights the top damage sites and their distribution between different residues of the structure. Radiation damage can be identified and quantified by calculating B_{damage} values derived from *B*-factor values using the RABDAM program [86,87]. B_{damage} is a metric allowing analysis of the increase in atomic *B*-factor values, which indicate chemical changes at a specific site. B_{net} is an overall atomic *B*-factor, a derivative of the (per-atom) B_{damage} metric that highlights in a single value the total extent of specific radiation damage suffered by an MX structure and allows objective analysis of it.

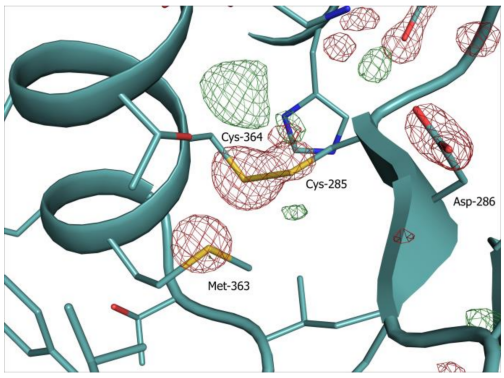

Figure 2. Difference density map presenting specific damage sites (cleavage of disulfide bridge, decarboxylation of aspartic acid and disordering of methionine sulfur) in GH7 family cellobiohydrolase, PDB: 5MCC [79]. $F_{\mathrm{obs(5)}}$–$F_{\mathrm{obs(1)}}$ Fourier difference maps between dataset 1 and 5 collected on the same crystal are shown, contoured at +/− 5 σ. Negative difference density (red) indicates electron density loss and the positive difference density (green) indicates electron density gain with increasing dose. The maps were calculated with RIDL [85] using the phases of the structure refined from dataset 1.

6. Conclusions

Radiation damage continues to be an intrinsic part of X-ray crystallography, but owing to continuous systematic research, significant progress has been made in our knowledge and understanding of it in MX. However, there are many stages in the MX pipeline where the experimental structural biologist can use the available information to mitigate or at least to take into account the possible effects, so that the best possible three-dimensional structure can be obtained and as accurate conclusions as possible can be drawn from it. This is summarised in Figure 3. It is vital to understand the interplay between the various experimental parameters and, in particular, the radiation-damage processes. Further systematic experiments are still required to enable us to optimize the use of the new 4th generation synchrotron produced X-ray beams as well as XFELs in order to solve the dilemma of the experimental structural biologist: diffraction before destruction.

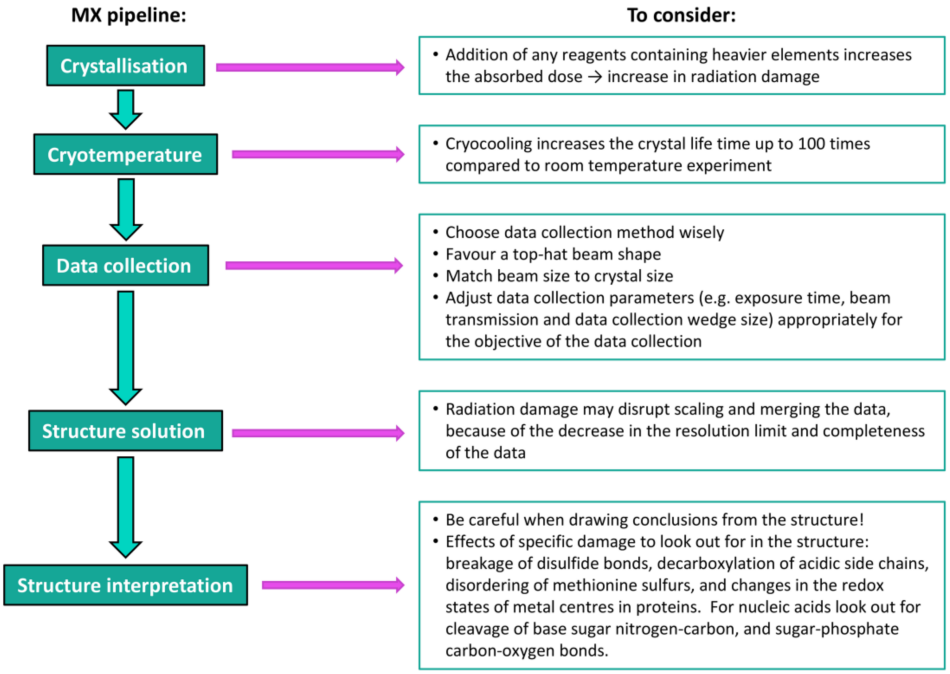

Figure 3. Flow chart to summarising the stages in the MX pipeline to be considered to minimise the radiation-induced damage in macromolecules.

Acknowledgments: I wish to gratefully acknowledge Elspeth Garman for all her help in preparing this manuscript and Charles Bury for his help in making the figures. This work was supported by the Finnish Cultural Foundation.

Conflicts of Interest: The author declares no conflict of interest. The founding sponsor had no role in the design of the study; in the collection, analyses, or interpretation of data; in the writing of the manuscript, and in the decision to publish the results.

References

1. Blake, C.C.F.; Phillips, D.C. Effects of X-irradiation on single crystals of myoglobin. In *Biological Effects of Ionizing Radiation at the Molecular Level*; International Atomic Energy Agency: Vienna, Austria, 1962; pp. 183–191.
2. Ravelli, R.B.; McSweeney, S.M. The 'fingerprint' that X-rays can leave on structures. *Structure* **2000**, *8*, 315–328. [CrossRef]
3. Weik, M.; Ravelli, R.B.; Kryger, G.; McSweeney, S.; Raves, M.L.; Harel, M.; Gros, P.; Silman, I.; Kroon, J.; Sussman, J.L. Specific chemical and structural damage to proteins produced by synchrotron radiation. *Proc. Natl. Acad. Sci. USA* **2000**, *97*, 623–628. [CrossRef] [PubMed]

4. Murray, J.; Garman, E. Investigation of possible free-radical scavengers and metrics for radiation damage in protein cryocrystallography. *J. Synchrotron Radiat.* **2002**, *9*, 347–354. [CrossRef] [PubMed]
5. Burmeister, W.P. Structural changes in a cryo-cooled protein crystal owing to radiation damage. *Acta Crystallogr. Sect. D Biol. Crystallogr.* **2000**, *56*, 328–341. [CrossRef]
6. Carugo, O.; Carugo, K.D. When X-rays modify the protein structure: Radiation damage at work. *Trends Biochem. Sci.* **2005**, *30*, 213–219. [CrossRef] [PubMed]
7. Weiss, M.S.; Panjikar, S.; Mueller-Dieckmann, C.; Tucker, P.A. On the influence of the incident photon energy on the radiation damage in crystalline biological samples. *J. Synchrotron Radiat.* **2005**, *12*, 304–309. [CrossRef] [PubMed]
8. Corbett, M.C.; Latimer, M.J.; Poulos, T.L.; Sevrioukova, I.F.; Hodgson, K.O.; Hedman, B. Photoreduction of the active site of the metalloprotein putidaredoxin by synchrotron radiation. *Acta Crystallogr. Sect. D Biol. Crystallogr.* **2007**, *63*, 951–960. [CrossRef] [PubMed]
9. Garman, E.F. Radiation damage in macromolecular crystallography: What is it and why should we care? *Acta Crystallogr. Sect. D Biol. Crystallogr.* **2010**, *66*, 339–351. [CrossRef] [PubMed]
10. Dubnovitsky, A.P.; Ravelli, R.B.; Popov, A.N.; Papageorgiou, A.C. Strain relief at the active site of phosphoserine aminotransferase induced by radiation damage. *Protein Sci.* **2005**, *14*, 1498–1507. [CrossRef] [PubMed]
11. Murray, J.W.; Rudino-Pinera, E.; Owen, R.L.; Grininger, M.; Ravelli, R.B.; Garman, E.F. Parameters affecting the X-ray dose absorbed by macromolecular crystals. *J. Synchrotron Radiat.* **2005**, *12*, 268–275. [CrossRef] [PubMed]
12. Fioravanti, E.; Vellieux, F.M.; Amara, P.; Madern, D.; Weik, M. Specific radiation damage to acidic residues and its relation to their chemical and structural environment. *J. Synchrotron Radiat.* **2007**, *14*, 84–91. [CrossRef] [PubMed]
13. McCoy, A.J.; Read, R.J. Experimental phasing: Best practice and pitfalls. *Acta Crystallogr. Sect. D Biol. Crystallogr.* **2010**, *66*, 458–469. [CrossRef] [PubMed]
14. Schmidt, M.; Šrajer, V.; Purwar, N.; Tripathi, S. The kinetic dose limit in room-temperature time-resolved macromolecular crystallography. *J. Synchrotron Radiat.* **2012**, *19*, 264–273. [CrossRef] [PubMed]
15. Matsui, Y.; Sakai, K.; Murakami, M.; Shiro, Y.; Adachi, S.; Okumura, H.; Kouyama, T. Specific damage induced by X-ray radiation and structural changes in the primary photoreaction of bacteriorhodopsin. *J. Mol. Biol.* **2002**, *324*, 469–481. [CrossRef]
16. Hope, H. Cryocrystallography of biological macromolecules: A generally applicable method. *Acta Crystallogr. Sect. B Struct. Sci. Cryst. Eng. Mater.* **1988**, *44*, 22–26. [CrossRef]
17. Teng, T. Mounting of crystals for macromolecular crystallography in a free-standing thin film. *J. Appl. Crystallogr.* **1990**, *23*, 387–391. [CrossRef]
18. Garman, E.F.; Schneider, T.R. Macromolecular cryocrystallography. *J. Appl. Crystallogr.* **1997**, *30*, 211–237. [CrossRef]
19. Garman, E. Cool data: Quantity AND quality. *Acta Crystallogr. Sect. D Biol. Crystallogr.* **1999**, *55*, 1641–1653. [CrossRef]
20. Nave, C.; Garman, E.F. Towards an understanding of radiation damage in cryocooled macromolecular crystals. *J. Synchrotron Radiat.* **2005**, *12*, 257–260. [CrossRef] [PubMed]
21. Allan, E.G.; Kander, M.C.; Carmichael, I.; Garman, E.F. To scavenge or not to scavenge, that is STILL the question. *J. Synchrotron Radiat.* **2013**, *20*, 23–36. [CrossRef] [PubMed]
22. Ravelli, R.B.; Garman, E.F. Radiation damage in macromolecular cryocrystallography. *Curr. Opin. Struct. Biol.* **2006**, *16*, 624–629. [CrossRef] [PubMed]
23. Bourenkov, G.P.; Popov, A.N. Optimization of data collection taking radiation damage into account. *Acta Crystallogr. Sect. D Biol. Crystallogr.* **2010**, *66*, 409–419. [CrossRef] [PubMed]
24. Kmetko, J.; Husseini, N.S.; Naides, M.; Kalinin, Y.; Thorne, R.E. Quantifying X-ray radiation damage in protein crystals at cryogenic temperatures. *Acta Crystallogr. Sect. D Biol. Crystallogr.* **2006**, *62*, 1030–1038. [CrossRef] [PubMed]
25. Owen, R.L.; Rudino-Pinera, E.; Garman, E.F. Experimental determination of the radiation dose limit for cryocooled protein crystals. *Proc. Natl. Acad. Sci. USA* **2006**, *103*, 4912–4917. [CrossRef] [PubMed]
26. Sliz, P.; Harrison, S.C.; Rosenbaum, G. How does radiation damage in protein crystals depend on X-ray dose? *Structure* **2003**, *11*, 13–19. [CrossRef]

27. Leiros, H.; Timmins, J.; Ravelli, R.B.; Mcsweeney, S.M. Is radiation damage dependent on the dose rate used during macromolecular crystallography data collection? *Acta Crystallogr. Sect. D Biol. Crystallogr.* **2006**, *62*, 125–132. [CrossRef] [PubMed]
28. Paithankar, K.S.; Garman, E.F. Know your dose: RADDOSE. *Acta Crystallogr. Sect. D Biol. Crystallogr.* **2010**, *66*, 381–388. [CrossRef] [PubMed]
29. Garman, E.F.; Owen, R.L. Cryocooling and radiation damage in macromolecular crystallography. *Acta Crystallogr. Sect. D Biol. Crystallogr.* **2006**, *62*, 32–47. [CrossRef] [PubMed]
30. Southworth-Davies, R.J.; Garman, E.F. Radioprotectant screening for cryocrystallography. *J. Synchrotron Radiat.* **2007**, *14*, 73–83. [CrossRef] [PubMed]
31. Nowak, E.; Brzuszkiewicz, A.; Dauter, M.; Dauter, Z.; Rosenbaum, G. To scavenge or not to scavenge: That is the question. *Acta Crystallogr. Sect. D Biol. Crystallogr.* **2009**, *65*, 1004–1006. [CrossRef] [PubMed]
32. Kmetko, J.; Warkentin, M.; Englich, U.; Thorne, R.E. Can radiation damage to protein crystals be reduced using small-molecule compounds? *Acta Crystallogr. Sect. D Biol. Crystallogr.* **2011**, *67*, 881–893. [CrossRef] [PubMed]
33. De la Mora, E.; Carmichael, I.; Garman, E.F. Effective scavenging at cryotemperatures: Further increasing the dose tolerance of protein crystals. *J. Synchrotron Radiat.* **2011**, *18*, 346–357. [CrossRef] [PubMed]
34. Barker, A.I.; Southworth-Davies, R.J.; Paithankar, K.S.; Carmichael, I.; Garman, E.F. Room-temperature scavengers for macromolecular crystallography: Increased lifetimes and modified dose dependence of the intensity decay. *J. Synchrotron Radiat.* **2009**, *16*, 205–216. [CrossRef] [PubMed]
35. Holton, J.M. A beginner's guide to radiation damage. *J. Synchrotron Radiat.* **2009**, *16*, 133–142. [CrossRef] [PubMed]
36. Holton, J.M.; Frankel, K.A. The minimum crystal size needed for a complete diffraction data set. *Acta Crystallogr. Sect. D Biol. Crystallogr.* **2010**, *66*, 393–408. [CrossRef] [PubMed]
37. Garman, E.F.; Weik, M. Radiation Damage in Macromolecular Crystallography. In *Protein Crystallography: Methods and Protocols*; Wlodawer, A., Dauter, Z., Jaskolski, M., Eds.; Springer Nature: New York, NY, USA, 2017; pp. 467–489.
38. Fraser, J.S.; van den Bedem, H.; Samelson, A.J.; Lang, P.T.; Holton, J.M.; Echols, N.; Alber, T. Accessing protein conformational ensembles using room-temperature X-ray crystallography. *Proc. Natl. Acad. Sci. USA* **2011**, *108*, 16247–16252. [CrossRef] [PubMed]
39. Owen, R.L.; Axford, D.; Nettleship, J.E.; Owens, R.J.; Robinson, J.I.; Morgan, A.W.; Doré, A.S.; Lebon, G.; Tate, C.G.; Fry, E.E. Outrunning free radicals in room-temperature macromolecular crystallography. *Acta Crystallogr. Sect. D Biol. Crystallogr.* **2012**, *68*, 810–818. [CrossRef] [PubMed]
40. Gati, C.; Bourenkov, G.; Klinge, M.; Rehders, D.; Stellato, F.; Oberthür, D.; Yefanov, O.; Sommer, B.P.; Mogk, S.; Duszenko, M. Serial crystallography on in vivo grown microcrystals using synchrotron radiation. *IUCrJ* **2014**, *1*, 87–94. [CrossRef] [PubMed]
41. Standfuss, J.; Spence, J. Serial crystallography at synchrotrons and X-ray lasers. *IUCrJ* **2017**, *4*, 100–101. [CrossRef] [PubMed]
42. Warkentin, M.; Hopkins, J.B.; Badeau, R.; Mulichak, A.M.; Keefe, L.J.; Thorne, R.E. Global radiation damage: Temperature dependence, time dependence and how to outrun it. *J. Synchrotron Radiat.* **2013**, *20*, 7–13. [CrossRef] [PubMed]
43. Pflugrath, J. Macromolecular cryocrystallography—Methods for cooling and mounting protein crystals at cryogenic temperatures. *Methods* **2004**, *34*, 415–423. [CrossRef] [PubMed]
44. Zeldin, O.B.; Gerstel, M.; Garman, E.F. RADDOSE-3D: Time-and space-resolved modelling of dose in macromolecular crystallography. *J. Appl. Crystallogr.* **2013**, *46*, 1225–1230. [CrossRef]
45. Bury, C.S.; Brooks-Bartlett, J.C.; Walsh, S.P.; Garman, E.F. Estimate your dose: RADDOSE-3D. *Protein Sci.* **2018**, *27*, 217–228. [CrossRef] [PubMed]
46. Nave, C. Radiation damage in protein crystallography. *Radiat. Phys. Chem.* **1995**, *45*, 483–490. [CrossRef]
47. Sanishvili, R.; Yoder, D.W.; Pothineni, S.B.; Rosenbaum, G.; Xu, S.; Vogt, S.; Stepanov, S.; Makarov, O.A.; Corcoran, S.; Benn, R.; et al. Radiation damage in protein crystals is reduced with a micron-sized X-ray beam. *Proc. Natl. Acad. Sci. USA* **2011**, *108*, 6127–6132. [CrossRef] [PubMed]
48. Krause, M.O. Atomic radiative and radiationless yields for *K* and *L* shells. *J. Phys. Chem. Ref. Data* **1979**, *8*, 307–327. [CrossRef]

49. O'Neill, P.; Stevens, D.L.; Garman, E.F. Physical and chemical considerations of damage induced in protein crystals by synchrotron radiation: A radiation chemical perspective. *J. Synchrotron Radiat.* **2002**, *9*, 329–332. [CrossRef] [PubMed]
50. Nave, C.; Hill, M.A. Will reduced radiation damage occur with very small crystals? *J. Synchrotron Radiat.* **2005**, *12*, 299–303. [CrossRef] [PubMed]
51. Jones, G.D.; Lea, J.S.; Symons, M.C.; Taiwo, F.A. Structure and mobility of electron gain and loss centres in proteins. *Nature* **1987**, *330*, 772–773. [CrossRef] [PubMed]
52. Taylor, G.L. Introduction to phasing. *Acta Crystallogr. Sect. D Biol. Crystallogr.* **2010**, *66*, 325–338. [CrossRef] [PubMed]
53. Dodson, E. The befores and afters of molecular replacement. *Acta Crystallogr. Sect. D Biol. Crystallogr.* **2008**, *64*, 17–24. [CrossRef] [PubMed]
54. Vijayan, M.; Ramaseshan, S. Isomorphous replacement and anomalous scattering. In *International Tables for Crystallography Volume B*; Shmueli, U., Ed.; Springer: Dordrecht, The Netherlands, 1993; pp. 264–275.
55. Schneider, T.R.; Sheldrick, G.M. Substructure solution with SHELXD. *Acta Crystallogr. Sect. D Biol. Crystallogr.* **2002**, *58*, 1772–1779. [CrossRef]
56. Sheldrick, G.M. A short history of SHELX. *Acta Crystalloger. Sect. A Found. Crystallogr.* **2008**, *64*, 112–122. [CrossRef] [PubMed]
57. Pike, A.C.; Garman, E.F.; Krojer, T.; von Delft, F.; Carpenter, E.P. An overview of heavy-atom derivatization of protein crystals. *Acta Crystallogr. Sect. D Biol. Crystallogr.* **2016**, *72*, 303–318. [CrossRef] [PubMed]
58. Gonzalez, A. Optimizing data collection for structure determination. *Acta Crystallogr. Sect. D Biol. Crystallogr.* **2003**, *59*, 1935–1942. [CrossRef]
59. Schmidt, A.; Gonzalez, A.; Morris, R.J.; Costabel, M.; Alzari, P.M.; Lamzin, V.S. Advantages of high-resolution phasing: MAD to atomic resolution. *Acta Crystallogr. Sect. D Biol. Crystallogr.* **2002**, *58*, 1433–1441. [CrossRef] [PubMed]
60. González, A.; Delft, F.V.; Liddington, R.C.; Bakolitsa, C. Two-wavelength MAD phasing and radiation damage: A case study. *J. Synchrotron Radiat.* **2005**, *12*, 285–291. [CrossRef] [PubMed]
61. Rice, L.M.; Earnest, T.; Brunger, A.T. Single-wavelength anomalous diffraction phasing revisited. *Acta Crystallogr. Sect. D Biol. Crystallogr.* **2000**, *56*, 1413–1420. [CrossRef]
62. González, A. A comparison of SAD and two-wavelength MAD phasing for radiation-damaged Se-MET crystals. *J. Synchrotron Radiat.* **2007**, *14*, 43–50. [CrossRef] [PubMed]
63. Ravelli, R.B.; Leiros, H.S.; Pan, B.; Caffrey, M.; McSweeney, S. Specific radiation damage can be used to solve macromolecular crystal structures. *Structure* **2003**, *11*, 217–224. [CrossRef]
64. Weiss, M.S.; Mander, G.; Hedderich, R.; Diederichs, K.; Ermler, U.; Warkentin, E. Determination of a novel structure by a combination of long-wavelength sulfur phasing and radiation-damage-induced phasing. *Acta Crystallogr. Sect. D Biol. Crystallogr.* **2004**, *60*, 686–695. [CrossRef] [PubMed]
65. Shimizu, N.; Hirata, K.; Hasegawa, K.; Ueno, G.; Yamamoto, M. Dose dependence of radiation damage for protein crystals studied at various X-ray energies. *J. Synchrotron Radiat.* **2007**, *14*, 4–10. [CrossRef] [PubMed]
66. Homer, C.; Cooper, L.; Gonzalez, A. Energy dependence of site-specific radiation damage in protein crystals. *J. Synchrotron Radiat.* **2011**, *18*, 338–345. [CrossRef] [PubMed]
67. Fourme, R.; Honkimäki, V.; Girard, E.; Medjoubi, K.; Dhaussy, A.; Kahn, R. Reduction of radiation damage and other benefits of short wavelengths for macromolecular crystallography data collection. *J. Appl. Crystallogr.* **2012**, *45*, 652–661. [CrossRef]
68. Liebschner, D.; Rosenbaum, G.; Dauter, M.; Dauter, Z. Radiation decay of thaumatin crystals at three X-ray energies. *Acta Crystallogr. Sect. D Biol. Crystallogr.* **2015**, *71*, 772–778. [CrossRef] [PubMed]
69. Schulze-Briese, C.; Wagner, A.; Tomizaki, T.; Oetiker, M. Beam-size effects in radiation damage in insulin and thaumatin crystals. *J. Synchrotron Radiat.* **2005**, *12*, 261–267. [CrossRef] [PubMed]
70. Bourenkov, G.P.; Popov, A.N. A quantitative approach to data-collection strategies. *Acta Crystallogr. Sect. D Biol. Crystallogr.* **2006**, *62*, 58–64. [CrossRef] [PubMed]
71. Schneider, T.R. Synchrotron radiation: Micrometer-sized X-ray beams as fine tools for macromolecular crystallography. *HFSP J.* **2008**, *2*, 302–306. [CrossRef] [PubMed]
72. Krojer, T.; von Delft, F. Assessment of radiation damage behaviour in a large collection of empirically optimized datasets highlights the importance of unmeasured complicating effects. *J. Synchrotron Radiat.* **2011**, *18*, 387–397. [CrossRef] [PubMed]

73. Berglund, G.I.; Carlsson, G.H.; Smith, A.T.; Szöke, H.; Henriksen, A.; Hajdu, J. The catalytic pathway of horseradish peroxidase at high resolution. *Nature* **2002**, *417*, 463. [CrossRef] [PubMed]
74. Polsinelli, I.; Savko, M.; Rouanet-Mehouas, C.; Ciccone, L.; Nencetti, S.; Orlandini, E.; Stura, E.A.; Shepard, W. Comparison of helical scan and standard rotation methods in single-crystal X-ray data collection strategies. *J. Synchrotron Radiat.* **2017**, *24*, 42–52. [CrossRef] [PubMed]
75. Kabsch, W. XDS. *Acta Crystallogr. Sect. D Biol. Crystallogr.* **2010**, *D66*, 125–132. [CrossRef] [PubMed]
76. Waterman, D.G.; Winter, G.; Gildea, R.J.; Parkhurst, J.M.; Brewster, A.S.; Sauter, N.K.; Evans, G. Diffraction-geometry refinement in the DIALS framework. *Acta Crystallogr. Sect. D Biol. Crystallogr.* **2016**, *72*, 558–575. [CrossRef] [PubMed]
77. Teng, T.Y.; Moffat, K. Primary radiation damage of protein crystals by an intense synchrotron X-ray beam. *J. Synchrotron Radiat.* **2000**, *7*, 313–317. [CrossRef] [PubMed]
78. Sutton, K.A.; Black, P.J.; Mercer, K.R.; Garman, E.F.; Owen, R.L.; Snell, E.H.; Bernhard, W.A. Insights into the mechanism of X-ray-induced disulfide-bond cleavage in lysozyme crystals based on EPR, optical absorption and X-ray diffraction studies. *Acta Crystallogr. Sect. D Biol. Crystallogr.* **2013**, *69*, 2381–2394. [CrossRef] [PubMed]
79. Bury, C.S.; Carmichael, I.; Garman, E.F. OH cleavage from tyrosine: Debunking a myth. *J. Synchrotron Radiat.* **2017**, *24*, 7–18. [CrossRef] [PubMed]
80. Kort, R.; Hellingwerf, K.J.; Ravelli, R.B. Initial events in the photocycle of photoactive yellow protein. *J. Biol. Chem.* **2004**, *279*, 26417–26424. [CrossRef] [PubMed]
81. Aoyama, H.; Muramoto, K.; Shinzawa-Itoh, K.; Hirata, K.; Yamashita, E.; Tsukihara, T.; Ogura, T.; Yoshikawa, S. A peroxide bridge between Fe and Cu ions in the O_2 reduction site of fully oxidized cytochrome c oxidase could suppress the proton pump. *Proc. Natl. Acad. Sci. USA* **2009**, *106*, 2165–2169. [CrossRef] [PubMed]
82. Bury, C.; Garman, E.F.; Ginn, H.M.; Ravelli, R.B.; Carmichael, I.; Kneale, G.; McGeehan, J.E. Radiation damage to nucleoprotein complexes in macromolecular crystallography. *J. Synchrotron Radiat.* **2015**, *22*, 213–224. [CrossRef] [PubMed]
83. Bury, C.S.; McGeehan, J.E.; Antson, A.A.; Carmichael, I.; Gerstel, M.; Shevtsov, M.B.; Garman, E.F. RNA protects a nucleoprotein complex against radiation damage. *Acta Crystallogr. Sect. D Biol. Crystallogr.* **2016**, *72*, 648–657. [CrossRef] [PubMed]
84. Ten Eyck, L.F. Crystallographic fast Fourier transforms. *Acta Crystallogr. Sect A Cryst. Phys. Diffr. Theor. Gen. Crystallogr.* **1973**, *29*, 183–191. [CrossRef]
85. Bury, C.S.; Garman, E.F. RIDL: A tool to investigate Radiation-Induced Density Loss. *J. Appl. Crystallogr.* **2018**, in press.
86. Gerstel, M.; Deane, C.M.; Garman, E.F. Identifying and quantifying radiation damage at the atomic level. *J. Synchrotron Radiat.* **2015**, *22*, 201–212. [CrossRef] [PubMed]
87. Shelley, K.L.; Dixon, T.P.E.; Brooks-Bartlett, J.C.; Garman, E.F. RABDAM: Quantifying specific radiation damage in individual protein crystal structures. *J. Appl. Crystallogr.* **2018**, *51*, 552–559. [CrossRef]